Global and Planetary Change 206 (2021) 103638

Contents lists available at ScienceDirect

Global and Planetary Change

journal homepage: www.elsevier.com/locate/gloplacha

Evolution of Arctic Ocean surface circulation from 1958 to 2017

Yilin Yang[a], Yuanzhi Zhang[a,b,*], X. San Liang[a], Qiuming Cheng[c], Jin Yeu Tsou[b,d]

[a] Nanjing University of Information Science and Technology, School of Marine Sciences, Nanjing 210044, China
[b] Chinese University of Hong Kong, Faculty of Social Science, Center for Housing Innovations and Institute of Asia-Pacific Studies, Shatin, Hong Kong
[c] Sun Yat-sen University, School of Earth Sciences and Engineering, Zhuhai 519000, China
[d] City University of Hong Kong, Department of Architecture and Civil Engineering, Hong Kong

ARTICLE INFO

Editor: Howard Falcon-Lang

Keywords:
Arctic Ocean surface circulation
SLP
SSH
EOF
Arctic Oscillation

ABSTRACT

Arctic Ocean surface circulation plays an important role in the global ocean circulation system. In recent years, its position and velocity have been changing constantly, attracting increasing attention. The cause of this change, however, is still a matter of disagreement. In this paper, we use empirical orthogonal function analysis (EOF) to analyze the spatial and temporal distributions of sea level pressure (SLP), sea surface height (SSH) and sea surface temperature (SST) in the Arctic Ocean. We use the wavelet transform to obtain the periodic variation law governing Arctic Ocean surface circulation as well as to explore the relationship between the Arctic Oscillation (AO) and Arctic Ocean surface circulation. Our results show that the SSH of the Arctic Ocean exhibit a periodic variation with AO, in particular the sudden change seen from 1987 to 1992 coinciding with the trend of the AO index for the same period. When the AO index is positive, the Beaufort Gyre (BG) weakens and the source of transpolar drift (TPD) moves eastward, to the East Siberian Sea; when the AO index is negative, the BG accelerates and expands and the source of TPD moves to the New Siberian Islands. As a result, the direction and amplitude of the circulation change.

1. Introduction

In recent years, a growing focus on climate change has drawn increasing attention to the Arctic Ocean, whose circulation is an important part of the global ocean circulation and is governed by wind stress, temperature, salt, and the atmosphere, among other factors. Although the Arctic Ocean is small and land-locked, it plays an important role in the circulation of other oceans and even the global ocean circulation in this pattern of seawater exchange. Climate models indicate that increased freshwater outflow from the Arctic may reduce convection in the North Atlantic deep water formation regions, which in turn may affects the Atlantic meridional overturning circulation (Wadley and Bigg, 2002). The Arctic is most remarkable for its perennial sea ice, which historically covered about half the Arctic Ocean, although the latest research shows that the Arctic sea ice has decreased by 2.22 million km^2 in the past 40 years (Simmonds and Li, 2021). Declining sea ice has profound implications for global climate change (Nghiem et al., 2007). The research of Luo et al. (2018a) on high-latitude European blocking and Ural blocking events shows that the cooling in Europe and central-eastern Asia are both related to the decrease of sea ice concentration. In recent years, under the influence of sea surface temperature (SST), atmosphere, and the Arctic Oscillation and other factors, the path and speed of Arctic circulation have changed significantly, affecting both the environment and the climate around the Arctic and playing an important role in the study of global ocean cycle and climate change.

Surface circulation in the Arctic Ocean comprises mainly transpolar drift (TPD) and the Beaufort Gyre (BG). TPD originates with river runoff in Siberia, with the surface water in the Arctic moving eastward with a westerly wind and flowing into the Atlantic Ocean along the east coast of Greenland. The BG, an anticyclonic circulation in the Beaufort Sea, plays an important role in the changes seen in the upper ocean, rotating the surface water in the Canadian Basin and causing the Arctic Sea ice to rotate with it (Zhong et al., 2015). Additionally, the BG exhibits clear seasonal and interannual variations.

A hydrographic survey of the Arctic Ocean in 1993 shows that the position of the Arctic circulation had changed since the early 1990s, with the intersection of the Pacific and Atlantic waters having moved from Lomonosov Ridge to Alpha-Mendeleyev Ridge, calling for a change to the upper ocean circulation model (Morison et al., 1998). Proshutinsky and Johnson (2001) identified two regimes of wind-forced circulation in the Arctic Ocean that may help explain recently observed significant basin-scale changes in the Arctic's temperature and salinity

* Corresponding author at: Nanjing University of Information Science and Technology, School of Marine Sciences, Nanjing 210044, China.
E-mail address: yuanzhizhang@cuhk.edu.hk (Y. Zhang).

https://doi.org/10.1016/j.gloplacha.2021.103638
Received 24 February 2021; Received in revised form 12 August 2021; Accepted 3 September 2021
Available online 9 September 2021

structure as well as the variability of ice conditions in the Arctic Ocean. Karcher et al. (2012) found that Ekman pumping in the Canadian Basin was extremely strong in the late 2000s, with the high freshwater content in the BG having restored some of the surface circulation to the level seen before the 1990s. After 2004, strong Ekman pumping in the Canadian Basin promoted the development of the BG and a new circulation mechanism appeared. Freshwater volume in the BG changes significantly on a seasonal and interannual scale, peaking from June to July and from November to January, with the freshwater center having shown a trend of southeast movement from 2003 to 2007. These changes are thought to be related to changes in wind stress curl, which affect circulation in the surface layer of the ocean through Ekman transport and cause the vertical movement of seawater. Recent studies have shown that the enhanced surface stress of the anticyclone over the BG is related to the deepening of the halocline and the accumulation of freshwater content (Ma et al., 2017). Krishfield et al. (2014) analyzed the perennial sea ice time series covering it from 2003 to 2012 and noted that sea ice content is decreasing. The study showed a decreasing trend of sea ice in the BG region, with older sea ice gradually melting and disappearing from the BG, which in turn led to changes in the freshwater content of the region. It will also impact on freshwater input and output at the same time. Zhong et al. (2015) believed that the BG had accelerated from 2003 to 2012, with upwelling dominant in most areas of the basin and northward Ekman transport released freshwater into the basin for many years indeed the total amount of Pacific winter water increased by 18% from 2002 to 2006 to 2011–2016. Changes in the BG are increasingly influencing changes to the upper ocean and climate (Zhong et al., 2019). The southeastern BG accelerated from late 2007 until 2011 and decreased to speeds near those seen in 2003–2006 (Armitage et al., 2018). Timokhov et al. (2018) showed that compared with 1949–1993, the pole crossing drift seen in 2007–2013 had become two branches: the first starting in the northern part of the Chukchi Sea and the second in the East Siberian Sea. The current bifurcation point was closer to the Canadian islands, with the flow rate increased by 1.5–2 times.

Arctic Oscillation (AO) is usually defined as the leading-mode of EOF of sea level pressure (SLP), and the main characteristic is the dipole structure with the direction of the south north along the latitude (Thompson and Wallace, 1998). Its interannual variations can significantly impact the surface air temperature anomalies over the Arctic, especially in the spatial pattern of temperature change from 1980s to 1990s (Rigor et al., 2002). In recent years, the influence of variations in the AO on the Arctic Ocean surface circulation has been widely discussed. Steele et al. (2008) analyzed ocean temperature profile data and satellite data and found that with decreases in the AO index, some parts of the Arctic Ocean cooled by about 0.5 °C every ten years from 1930 to 1965, whereas with increases in the AO index, these areas warmed during the period 1965–1995, a change particularly evident after 2000. In summer 2007, the SST anomaly reached as high as 5 °C, and it was found that when the AO index is high, the water in the Bering Sea passes directly through the Arctic Ocean by means of cross-stage drift, whereas when the AO index is low, the water in the Bering Sea is brought into the Beaufort circulation (Steele, 2004). Polyakov and Johnson (2000) showed that the SSTs of the Barents Sea and the Greenland–Iceland–Norway Sea in the Eastern Arctic were higher than average level in the 1950s but showed a downward trend until the 1960s, then returned to an upward trend in the following decades—a change consistent with low-frequency changes to the AO. Morison et al. (2012) showed that increased freshwater content in the Arctic Ocean was caused by forced atmospheric circulation accompanied by increases in the AO index. They also confirmed that runoff was an important factor affecting the Arctic Ocean, with spatiotemporal variations in its path affected by the AO rather than by wind-driven BG.

Atmosphere plays an intermediary role in the response of the Arctic Ocean to the AO, the troposphere and stratosphere as a medium make the loss of sea ice force AO to change (Screen et al., 2018; Sun et al., 2015). Nakamura et al. (2015) proved that the increase or decrease of Arctic sea ice area in November leads to more positive (negative) phases of AO in winter. This kind of connection is robust on the interannual and decadal time scales, so the weakening of AO and the corresponding mid-latitude climate change in recent years may be related to the sea ice loss in the Barents-Kara Sea (Yang et al., 2016). Changes in sea ice in the surface circulation can affect climate under sea-air-ice interactions. Chen et al. (2019); Luo et al. (2017); Luo et al. (2018b) revealed the influence of Ural blocking on the winter sea ice variability in the Barents-Kara Sea, and proposed that the combination of North Atlantic Oscillation -Ural blocking played a leading role in the reduction of BKS sea ice, and proposed the concept of "potential corticity barrier" to pointed out that the meridional potential vorticity gradient can better reflect the change of blocking duration related to Arctic warming. The abnormal circulation in the Arctic may cause extreme weather in the middle latitudes (Rudeva and Simmonds, 2021). Recent studies have shown that the East Asian cold anomaly is related to the sea ice loss in the Barents-Kara Sea and the atmospheric teleconnection patterns (Li et al., 2020). Decreases of sea ice from Barents-Kara Sea causes the tropospheric westerlies shift southward to significantly affect the winter climate and weather conditions in East Asia (Xu et al., 2021).

In this paper, we discuss changes to Arctic Ocean surface circulation from 1958 to 2017. The special geographical location and climatic conditions of the Arctic Ocean make exploration of the various characteristics of Arctic Ocean surface circulation essential to further understanding of global climate change.

2. Materials and methods

2.1. Study area

The study area is located in the entire Arctic Ocean within the Arctic Circle (66.5– 90°N, 0– 180°). Surrounded by North America and Eurasia, the Arctic Ocean connects with the Pacific Ocean through the Bering Strait and with the Atlantic Ocean through the Fram Strait. The presence of many river inlets into the marginal sea area lowers salinity, and the mixing process of the marginal sea and the Arctic Ocean water mass profoundly affects the properties of the Arctic ocean surface water. The external water inflow of the Arctic Ocean comes mainly from the freshwater input of the Pacific Ocean, the Atlantic Ocean, and rivers. The Arctic Ocean, which formed in response to multiple environmental factors associated with the Arctic, plays an important role in the global ocean circulation system and climate system. In the past 30 years, it has attracted increasing scholarly attention.

2.2. Datasets

2.2.1. ECMWF ORAS4 reanalysis datasets

In this paper, we use the data of Ocean Reanalysis System 4 (ORAS4) (Balmaseda et al., 2012) from European Centre for Medium-Range Weather Forecasts (ECMWF). The resolution of the data is 1° x 1°. This paper uses the data of salinity, zonal velocity, meridional velocity, and SSH with an interval of one month from 1958 to 2017.

2.2.2. NCEP\NCAR reanalysis datasets

The monthly reanalysis sea level pressure (SLP) data are from 1958 to 2017. The grid resolution is 2.5° × 2.5°.

2.2.3. ERSSTv5 datasets

Monthly sea surface temperature (SST) data from 1958 to 2017 were downloaded from the NOAA. The grid resolution is 2° × 2°.

2.3. Methods

2.3.1. Empirical orthogonal function analysis (EOF)

we use the empirical orthogonal function analysis (EOF) to decompose the sea level height (SSH) and sea surface temperature (SST) of the

Arctic Ocean. This is a method to analyze the structural features of matrix data and extract the main data features (Feng et al., 2019). It was first proposed by Pearson in 1902 and introduced into the analysis of meteorological problems by Lorenz (1956). This method takes the time series of the meteorological field as the analysis target and studies the temporal and spatial variation characteristics.

By the EOF, the original variable field can be represented by the linear combination of the temporal and spatial modes with the largest variance contribution. We used EOF to study SLP, SSH and SST in Arctic Ocean from 1958 to 2017 in this study.

2.3.2. *Wavelet coherence analysis (WTC)*

Wavelet coherence analysis (WTC) method is defined by Torrence and Compo (1998), which is used to calculate the common change region of two time series in time frequency space. The significance level of WTC is calculated by Monte Carlo method (Grinsted et al., 2004).

2.3.3. *Correlation analysis*

The Pearson correlation coefficient (Pearson, 1895) is used to measure the degree of correlation between two variables X and Y, and its value is between −1 to 1. In the field of natural science, the coefficient is widely used to measure the linear correlation between two variables (Ji et al., 2018). We use the Pearson correlation to calculate the spatial correlation between the SLP first and second mode time series and the Arctic Ocean SSH, so as to discuss the variation of the Arctic Ocean surface circulation.

3. Results

3.1. *Climatology analysis*

Fig. 1 shows a mean SST contour map of the Arctic Ocean from 1958 to 2017. The distribution of SST in the Arctic Ocean is relatively uniform. Because presence of sea ice limits surface water temperature, most of the temperature gradients in the Arctic Ocean basin are very small. Only in the Norway Sea and Barents Sea areas do the temperature gradients gradually increase, from north to south, in response to the injection of warmer water from the North Atlantic Ocean into the Arctic Ocean.

Fig. 2 shows the average salinity distribution of the Arctic Ocean. Due to the input of Atlantic and Pacific water and Siberian rivers, the stratification of Arctic Ocean water is mainly determined by salinity (Timmermans and Marshall, 2020). Significant spatial differences are seen in the salinity of the upper layer of the Arctic Ocean. The melting of large quantities of sea ice in the Canadian Basin and the input of Pacific water (Steele, 2004) and of freshwater from river runoff all produce low salinity in the upper layer. The input of freshwater from river runoff produces smaller salinity in the northern part of East Siberia, and the influence of Pacific water likewise lowers the upper salinity of the Makarov basin, whereas the Eurasian basin is less affected by the Pacific water and thus has a higher upper salinity—although the melting of sea ice in summer produces seasonal lows in the salinity of surface seawater.

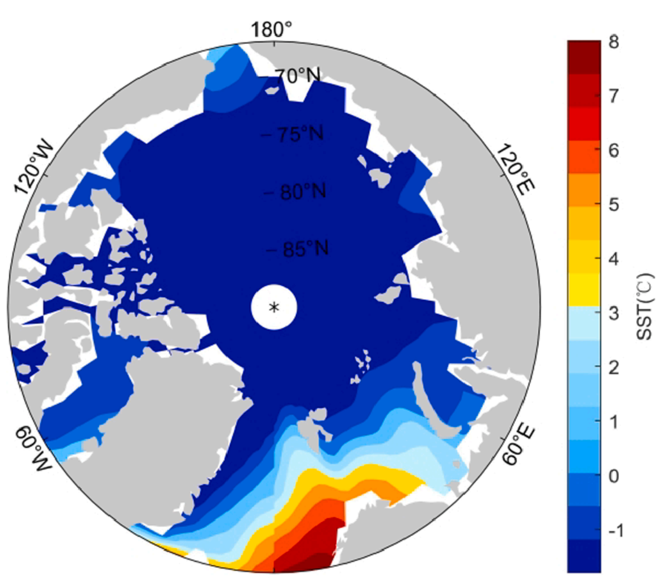

Fig. 1. Contour map of mean sea surface temperature in the Arctic Ocean from 1958 to 2017.

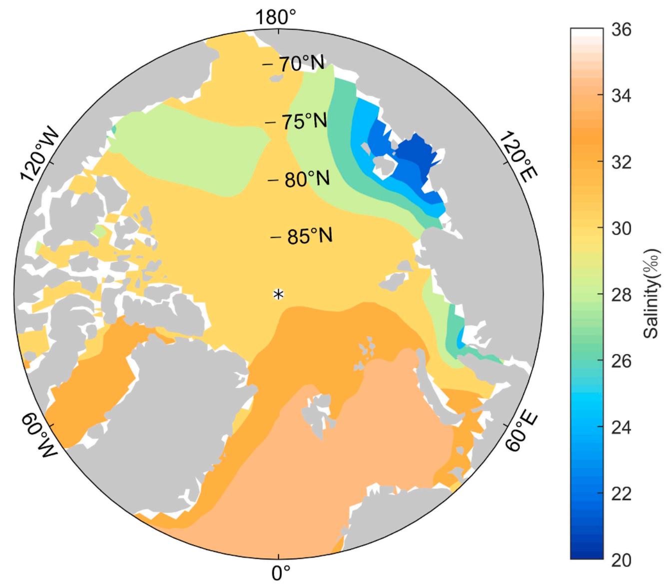

Fig. 2. Contour map of mean sea surface salinity in the Arctic Ocean from 1958 to 2017.

From 1958 to 2017, the SST of the Arctic Ocean has changed from −1 to 0 °C (Fig. 3), with a downward trend from the late 1950s to the 1960s and a gradual upward trend in the following decades. Sea surface salinity has fluctuated greatly, with two peaks in 1997–2007 and a sudden change to the minimum in 2008. Trends in SST and salinity in the Arctic Ocean have been essentially consistent, being inseparable from the changes in the Arctic Ocean's circulation, as discussed hereafter.

Fig. 4 shows the flow field map of the average SSH of the Arctic Ocean from 1958 to 2017, with the SSH of the Arctic Ocean gradually decreasing from the north pole of the Bering Strait toward the Norwegian Sea. Very clear closed circulation is seen between 120 and 180°W,

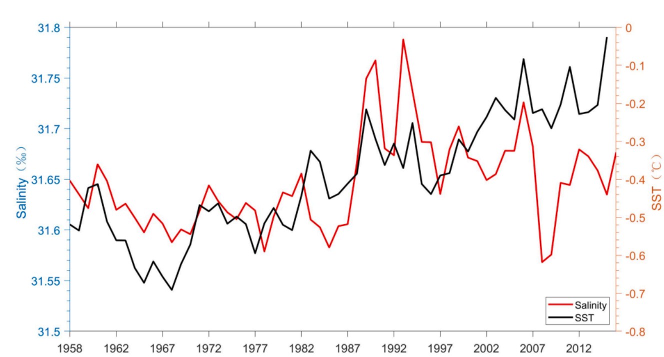

Fig. 3. The mean annual SST and salinity time series of the Arctic Ocean from 1958 to 2017 (the red curve is salinity and the black curve is SST). (For interpretation of the references to colour in this figure legend, the reader is referred to the web version of this article.)

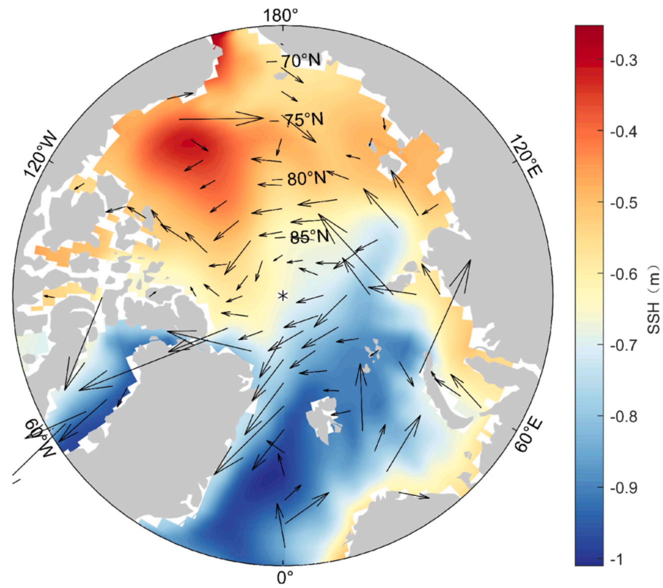

Fig. 4. Contour map of mean sea level height of superimposed flow field in the Arctic Ocean from 1958 to 2017 (unit: m/s).

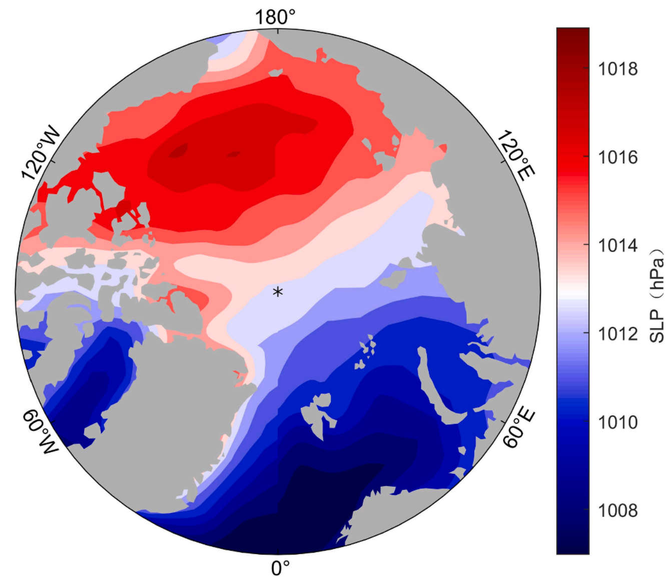

Fig. 5. Contour map of mean SLP in the Arctic Ocean from 1958 to 2017.

with the sea level at the circulation center higher but gradually decreasing toward the surrounding areas. The closed circulation at this position is associated with the BG, from the North Pacific through the Bering Strait. Flow velocity is larger in the inflow area than other area and gradually increases from the center toward the surrounding areas. The BG helps regulate Arctic climate change (Proshutinsky et al., 2002). The upwelling is dominant in the BG, which slowly rotates the surface water of the Canadian Basin. Northward Ekman transport will release the freshwater stored for many years in the basin and change the composition of the upper ocean (Zhong et al., 2015). There is a large area of Ekman downwelling in most parts of the Arctic Ocean under the wind stress curl mode, while there is a relatively strong upwelling in the northern European sea area (Timmermans and Marshall, 2020). In the blue area of the Fig. 4 the circulation seen moving along the contour line with relatively high velocity and large path curvature is TPD, which transports ice and water under the effects of the wind field. The current is driven eastward by Siberian river runoff and westerly winds. After describing a large bend in the northern European sea, it passes through the North Pole and flows rapidly into the Atlantic Ocean from the Canadian Arctic Archipelago and Greenland's Fram Strait.

The spatial distribution of mean SLP in Arctic Ocean shows that the highest SLP in the Arctic Ocean is 1018 hPa, and the lowest is 1008 hPa (Fig. 4). The high pressure area extends from the East Siberian Sea to the Canadian islands, and the low pressure area extends from the West Siberian Sea to Greenland. The Arctic Ocean SLP can reflect many characteristics of atmospheric circulation, such as the Arctic Oscillation and the Arctic dipole structure. It also has a strong seasonal variation and plays an important role in the study of climate and surface ocean change in the Arctic. We will make a detailed analysis of SLP in the following sections (Figs. 5 and 12).

3.2. Empirical orthogonal function (EOF) analysis

3.2.1. EOF analysis of sea level pressure (SLP) of Arctic Ocean

To explore the changes of the Arctic Ocean surface circulation, we use EOF to analyze the SLP in 66.5°N. We divide SLP monthly average data into winter semester (November to April) and summer semester (May to October) for EOF, and select the first two modes according to variance contribution rate. It is worth mentioning that PC1 in this paper is not a conventional AO mode. Different from the AO index of NOAA adopted by Simmonds et al. (2008), the AO index we defined is the time series of the main modes of EOF of SLP in winter and summer in the Arctic circle, while bearing that caveat in mind, we will subsequently refer to PC1 as the "AO". The first mode is the AO (Thompson and Wallace, 1998) mode and the second mode is the Arctic Dipole (AD) mode (Wu et al., 2004) from the two spatial distribution (Fig. 6), their corresponding time series are defined as AO index and AD index (Wang et al., 2009). We also analyzed the correlation between the first mode time series and the AO index provided by NOAA (National Oceanic and Atmospheric Administration) (https://www.cpc.ncep.noaa.gov/products/precip/CWlink/daily_ao_index/monthly.ao.index.b50.current.ascii.table). In the case of P value of 0.05, the correlation coefficient of AO index in winter is as high as 0.9069, and that in summer is 0.8407, which proves that our index is reliable and effective. The contribution rates of the variance of the first two modes of winter are 72.4% and 9.2% both pass the North-test with a confidence level of 95% (North et al., 1982).The first mode of SLP EOF in winter is negative in the north polar center, and shifts from the north pole point to the Siberia side. There are two abnormal centers in the second mode, one in the northern part of

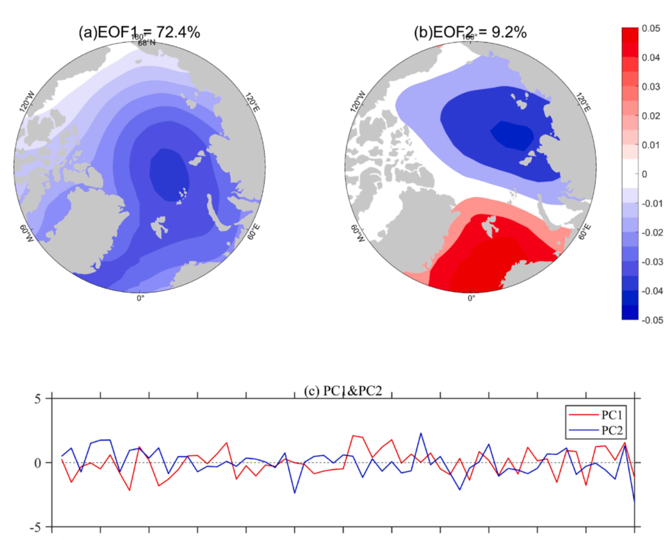

Fig. 6. The result of EOF analysis of winter SLP. The first mode (a), the second mode (b) spatial distribution, and time series (c) of the first mode and the second mode, all the time series have been standardized.

Siberia (Barents-Kara Sea) and the other in the North Atlantic and Greenland. There is an obvious dipole structure, which is more obvious in summer. (Fig. 7b). This distribution of SLP differences is beneficial to the flow and export of Arctic sea ice and surface water. From the time series, it can be seen that the winter AO index has been in a negative phase from 1975 to 1987, and suddenly turned to a positive phase from 1988 and lasted for several years. After that, AO index has been in a state of alternating positive and negative oscillation, and the amplitude is getting larger after 2008. In contrast, AD index fluctuated positively and negatively in winter, and peaked in 1982 and 1995. In recent years, the negative anomaly of SLP on the side of Barents-Kara Sea and the positive anomaly in Greenland and the North Atlantic region show a fluctuating trend.

The contribution rates of the variance of the first two modes of summer are 62.9% and 12.7% both pass the North-test with a confidence level of 95%. In summer (Fig. 7), the spatial distribution of the AO mode is closer to the north pole, and the negative anomaly decreases gradually from the center to the periphery area. The distribution of AD mode is more obvious in summer. The negative anomaly area is located in the whole sea area of northern Siberia, and the positive anomaly area is located in the sea area near Greenland and Canada islands. The distribution of positive and negative anomalies is roughly bounded by Bering Strait to Fram Strait. In the time series, AO index in summer fluctuated greatly from 1987 to 1995, and the AD index also changed from negative to positive at the same time. In addition, AD index maintained a high positive phase from 2015 to 2012.

3.2.2. EOF analysis of sea surface height (SSH) of Arctic Ocean

We used EOF to analyze temporal and spatial variations in SSH in the Arctic Ocean divided into winter and summer. Because the physical modes are not necessarily orthogonal, we must be cautious in interpreting the EOF results (Dommenget and Latif, 2002). The corresponding spatial distribution of SSH EOF analysis results describes the correlation of surface seawater physical properties, which is to say the correlation of seawater temperature and salinity. We selected the first mode of winter EOF and SSH in summer respectively, and the variance contribution rate reached 45.7% and 47.9% respectively. Both modes are passed the North-test with a confidence level of 95%.

The first mode (Fig. 8a, b) and its corresponding time series (Fig. 8c) of EOF clearly show that the SSH changes above the Eurasian basin and the upper continental shelf are inversely correlated. Both of the first modes are similar in winter and summer, indicating that there is no significant seasonal variation. The spatial of the first mode is related to

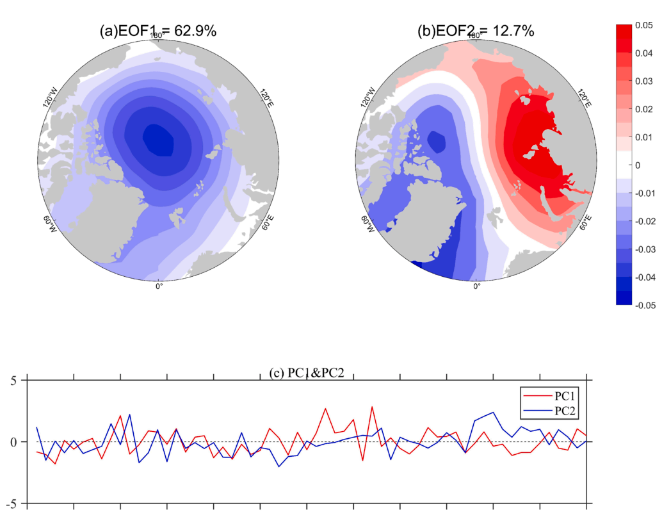

Fig. 7. The result of EOF analysis of summer SLP. The first mode (a), the second mode (b) spatial distribution, and time series (c) of the first and second mode, all the time series have been standardized.

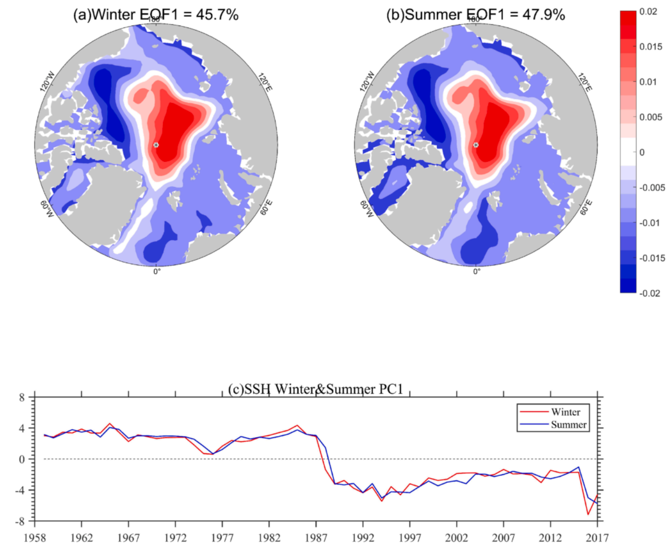

Fig. 8. Spatial distribution and time series of SSH EOF first mode in the Arctic Ocean: (a) the winter mode; (b) the summer mode; (c) time series of winter (red line) and summer (blue line), all the time series have been standardized. (For interpretation of the references to colour in this figure legend, the reader is referred to the web version of this article.)

the mixing of the water masses in the Arctic Ocean. The exchange of sea water between the Arctic Ocean and the North Atlantic has played a role in the process of sea water exchange, with which changes in the sea area above the Eurasian basin are positively correlated and changes in the sea area above the continental shelf negatively correlated. During 1958–1987, SSH above the Eurasian basin near the North Pole was abnormally high but SSH above the continental shelf abnormally low, whereas during 1988–2017, SSH above the Eurasian basin near the North Pole was abnormally low but SSH above the continental shelf abnormally high. The spatial distribution of the first mode shows a striking similarity of SSH change to the freshwater exchange pattern between the Arctic Ocean and the Atlantic.

During 1987– 1992, the first mode of EOF occurred in the interdecadal mutation, consistent with the annual average change of SSH. This mutation was confirmed by a hydrological survey of the Arctic Ocean in 1993: the position of the Arctic Ocean circulation has changed since the early 1990s, with the intersection of Pacific and Atlantic waters having moved from Lomonosov Ridge to Mendeleyev Ridge, calling for a change in the upper ocean circulation model (Morison et al., 1998). The reasons for this change are analyzed further hereafter. The first mode of SSH showed a clear upward trend during 2002– 2017, especially in the Beaufort Sea area. Beyond SSH rises caused by sea ice melting attributed to global warming, the rising trend also related to the acceleration of BG from 2000 to 2015. Upwelling dominated in most parts of the basin, and the northward Ekman transport released freshwater for many years, bringing changes in sea levels.

3.2.3. EOF analysis of sea surface temperature (SST) of Arctic Ocean

Although some studies have shown that the Arctic sea water is relatively cold, the ocean temperature could not strongly affect the ocean dynamic process, but with the trend of global warming, it still has an impact (Timmermans and Marshall, 2020). The EOF method is simultaneously used to analyze the SST seasonal distribution characteristics of the Arctic Ocean from 1958 to 2017. Fig. 9 show the first mode of SST in winter and summer and their corresponding time series and spatial distribution, which passed the North-test with a confidence level of 95%. The variance contribution rates of the winter and summer modes are 64.2% and 51.3%.

The first mode (Fig. 9a, b) and time series (Fig. 9c) indicate that SST changes in the Arctic Ocean are consistent, with all of them positive

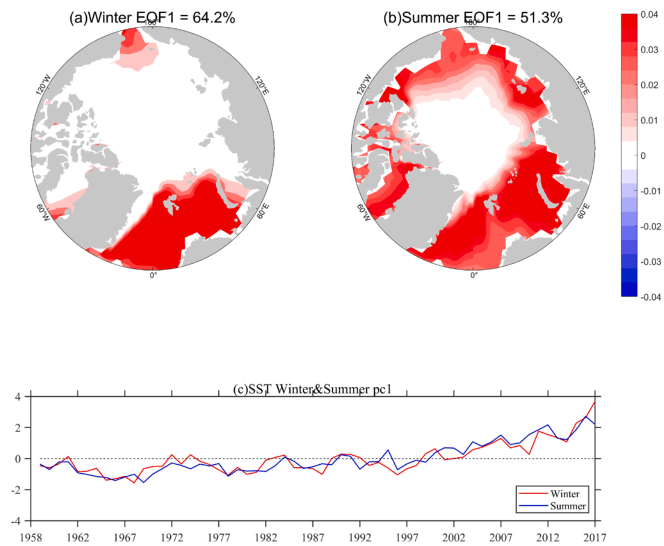

Fig. 9. Spatial distribution and time series of SST EOF first mode in the Arctic Ocean: (a) the winter mode; (b) the summer mode; (c) time series of winter (red line) and summer (blue line), all the time series have been standardized. (For interpretation of the references to colour in this figure legend, the reader is referred to the web version of this article.)

anomalies. The range of positive anomaly in summer is much larger than that in winter, which is due to the melting of sea ice in summer. The offshore waters of the Eurasian basin and the Canadian Basin are slightly weaker, and the continental margin is highly anomalous. This spatial distribution is thus likely caused by the input of freshwater from land and the mixing of seawater from the North Pacific and North Atlantic. Analysis shows that the North Atlantic subpolar gyre warmed in the 1990s and compensated for the cooling from the early 1960s to the mid-1990s (Chepurin and Carton, 2012). Combined with analysis of the spatial distribution map, it can be seen that the SST of the Arctic Ocean has increased gradually since the 2000s both in winter and summer. The increase of SST in the Arctic Ocean will accelerate the loss of sea ice, cause the accumulation of fresh water and the change of surface circulation in the Arctic Ocean, and affect the climate change in the surrounding and the middle latitudes areas.

3.3. The relationship between the Arctic Oscillation (AO) and Arctic circulation

The AO is the first principal component of the planetary scale atmospheric circulation variability. It reflects the north–south oscillation form of the reverse phase change of sea level pressure in the mid-latitude and Polar region, a process accompanied by atmospheric exchange. When the AO phase is positive, the pressure in the Arctic region is lower and the pressure in the middle latitude region outside the Arctic is higher; when the AO phase is negative, the pressure in the Arctic region is higher and the pressure in the middle latitude region is lower. Under the influence of the AO, the Arctic region is affected by primarily two wind patterns: The Beaufort high, with the Canadian Basin as its center, is anticyclonic, whereas the Icelandic low, outside the Arctic basin, is cyclonic (Timmermans and Marshall, 2020).

EOF analysis shows a regular relationship between the sea level changes in the Arctic Ocean of the past 60 years and meteorological and oceanic factors. The first mode of SSH shows two distinct closed loops. Thompson and Wallace (1998) thought this distribution pattern related to the AO and closely related to the exchange of seawater between the Arctic Ocean and the Atlantic Ocean.

At the same time, the AO index clearly underwent a sudden change from the negative phase to the positive phase during the period 1986–1990, which was negatively correlated with the annual average SSH change and change to the first mode of EOF for the same period. Thus an important relationship can be inferred between changes in both the Arctic Ocean's SSH and its circulation and the AO. In recent years, not only has the AO's strength increased, but so has its spatial structure. The polar vortex centers extend to the side of Greenland and the Bering Strait (Wang et al., 2015). Because this finding shows that the AO has a certain correlation with changes to the Arctic Ocean's surface circulation, we calculate the relationship between SSH and AO and other atmospheric circulation changes in the following section.

3.3.1. Wavelet coherence analysis

We calculated the first principal component (PC1) of SSH and the AO index in the winter and summer in time frequency space by WTC method (Fig. 10). The black thick line contour regions passed the significance test with a confidence level of 95%. The results show that the PC1 of SSH in winter is inversely correlated with AO index in 1966–1976, 1985–1995 and 2010–2014, especially in 1985–1995, the correlation coefficient is 0.9 on the time scale of 1–8 years (Fig. 10a). Previous studies have shown that the effect of AO in winter persisted for most of the following year (Rigor et al., 2002), and the large-scale ice anomaly in the summer of 1990 is related to the high frequency of cyclonic activity

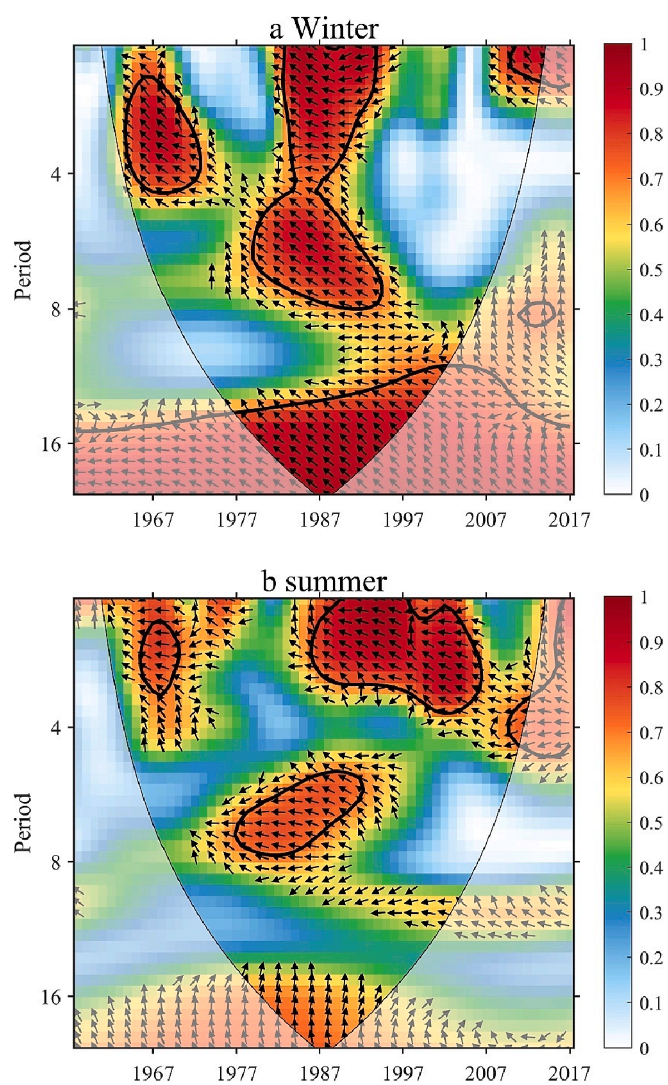

Fig. 10. The result of WTC between the SSH fist mode time series and the AO index in (a) winter and (b) summer. The black thick line contour regions passed the significance test with a confidence level of 95%. The thin line region is the influence cone. The leftward to the left indicates two time series are inversely correlated.

in spring (Serreze et al., 1995).

In summer, the time and period of the same change between PC1 and AO have changed, but in 1966–1968 and 1987–2006, they still show reverse correlation. Some studies have pointed out that the area of the perennial ice layer in 1990–1995 decreased by 9% compared with that in the previous decade, the sea ice loss can be related to the sharp increase in the frequency of the central Arctic low pressure system since 1989 (Maslanik et al., 1996). All the results have been showed that the variation of the surface circulation of the Arctic Ocean is closely related to AO and atmospheric circulation.

3.3.2. Spatial correlation between SSH and two leading modes of SLP

We also calculate the spatial correlation between SSH and two leading modes of SLP. As shown in Fig. 11, AO mode has a strong positive correlation with the change of SSH in the Arctic marginal sea area, which is more obvious in winter. AO signal changes most strongly in winter and early spring, when planetary waves in troposphere can propagate upward to Stratosphere (Thompson and Wallace, 2001). The positive phase of AO enhanced the runoff inflow in the Siberian marginal sea area, and more fresh water flowed into the Arctic Ocean, and entered the BG with the strong TPD. Although the Arctic Oscillation has a significant seasonal variation, its impact on SSH in the northern Siberian area is strong both in winter and summer. Among the dramatic changes in the Arctic Ocean in the 1990s, the sea ice loss in the northern Siberian Sea area is particularly serious (Maslanik et al., 1996).

Compared with AO, the impact of AD on SSH in the Arctic Ocean is weaker, but in summer, there is a significant positive correlation especially in the waters near to Greenland and the Canadian archipelago. The atmospheric circulation anomaly produces a strong meridional wind anomaly, which brings more sea ice from the west to the east of the Arctic Ocean to the North Atlantic (Wang et al., 2009). The long-term temperature anomaly and ice loss in western Greenland may be positively correlated with the change of AD (Overland et al., 2012).

3.4. Variation of surface circulation in the Arctic Ocean

We selected three typical periods of AO changes for analysis in Fig. 13. It can be seen that the variation of Arctic Ocean surface circulation with AO is more significant in summer.

3.4.1. The period of negative AO index (1967– 1971, 1977– 1982)

When the AO phase is negative, the BG gradually expands and accelerates and the source of TPD moved westward, to the Novosibirsk Islands. In summer most of the Bering Sea's warm water enters the Canadian Basin and drifts westward along the continental slope with the Alaskan coastal water, joining the gradually expanding BG, and a small part of the summer water enters TPD.

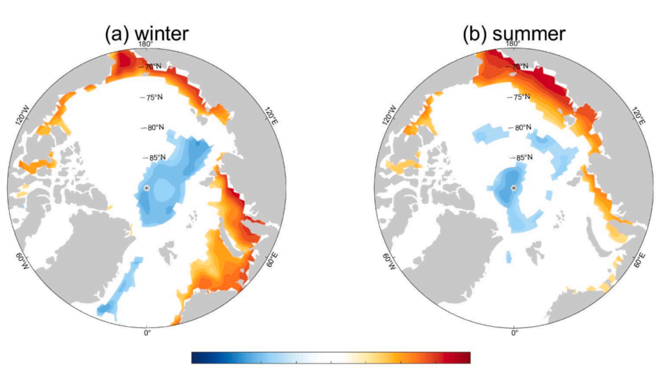

Fig. 11. Spatial Correlation of the AO mode of (a) winter monthly mean SLP (October–March) and (b) summer monthly mean SLP (April–September) with SSH, both with a *p*-value of 0.05.

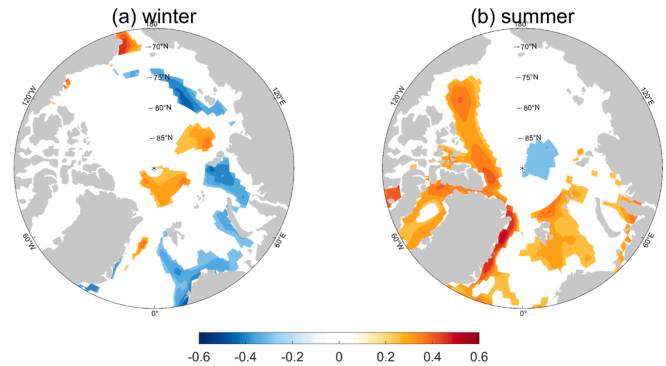

Fig. 12. Spatial Correlation of the AD mode of (a) winter monthly mean SLP (October–March) and (b) summer monthly mean SLP (April–September), both with a p-value of 0.05.

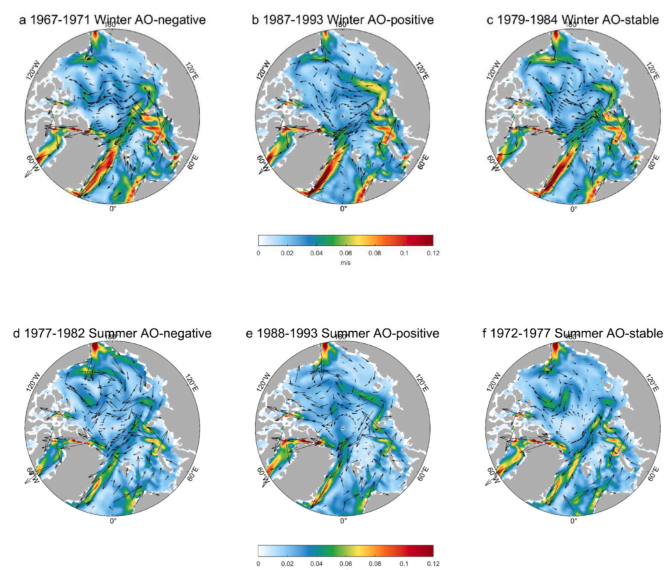

Fig. 13. Flow field diagram of positive AO index period in (a) winter and (d) summer, negative AO index period in (b) winter and (e) summer, stable AO index period in (c) winter and (f) summer., with the average velocity contour map (unit: m/s).

3.4.2. The period of positive AO index (1987– 1993, 1988– 1993)

When the AO index is in a significant positive phase, the BG in the Eastern Arctic Ocean is in a state of shrinking and weakening, which is caused by the mixing of vast quantities of sea water in the Western Arctic Ocean through TPD, the source of which moves eastward to the East Siberian Sea. Steele (2004) analyzed the evolution of Alaskan coastal water and Bering Sea summer warm water under different AO states and found that when AO is a strong positive phase, Alaskan coastal water was partially present above the continental shelf, flowing along it to the sea area near Greenland. The rest moved westward along the continental slope, mixed with the winter water of Bering Sea, entered the Canadian Basin to the east of the Chukchi Sea margin, and then entered the BG. At the same time, atmospheric circulation over the Eurasian basin became cyclonic, forcing the Siberian tributary shelf water of TPD drifting into the Makarov basin and the weakening BG.

3.4.3. The period of stable change of AO index (1979– 1984, 1972– 1977)

In the winter of 1979 to 1984 and the summer of 1972 to 1977, the AO index were in a stable state, so that changes to Arctic circulation varied between positive and negative periods: the source of TPD moved to the Novosibirsk Islands but still with a certain distance from the source of the negative phase, and with the strengthening of the westerly wind in the Chukchi Sea and the sea area north of Canada, seawater and sea ice began to drift westward again, supplementing the BG.

4. Discussion

In this paper, we used EOF to analyze the seasonal temporal and spatial distribution characteristics of SLP, SSH and SST in the Arctic Ocean and used correlation analysis to assess periodic variations in Arctic Ocean surface circulation with the change of SLP leading modes. Simultaneously, we explored the relationship between the AO and Arctic Ocean surface circulation.

EOF analysis shows relatively stable changes to Arctic Ocean SSH before 1987 and after 1992, with a sudden change seen between 1987 and 1992. Before and after that change, the direction of the Pacific water entering the Arctic Ocean from the Bering Strait also changed, as did SST and salinity. Our results show that the SSH of the Arctic Ocean exhibit a periodic variation with AO. After the 1990s, the Arctic Ocean has seen a sudden change, with circulation beginning to change significantly. This change is closely related to the AO. When the AO index is in a positive phase, the westerly wind is weak and the BG is weakened, so that freshwater remains in the BG and the source of TPD moves eastward to the East Siberian Sea. By contrast, when the AO index is in a negative phase, the westerly wind is strong and the BG accelerates and expands, so that the source of TPD moves to the Novosibirsk Islands, changing the circulatory path.

5. Conclusions

Arctic Ocean surface circulation, an important part of global oceanic circulation, and it arises in response to multiple factors, such as wind stress, temperature and salinity, atmosphere, and so on. At present, the Arctic Ocean surface circulation path, evolutionary mechanism, and many other issues have not been solved at a fundamental level, and because the Arctic atmosphere and ocean circulation have been changing, further observation and study are needed.

Changes to AO are of significant reference value for study of changes to Arctic Ocean surface circulation. AO affects the atmospheric circulation and then oceanic circulation, changing the position and velocity of Arctic Ocean surface circulation and changing the hydrological elements of the Arctic Ocean. The response mechanism and law between the AO and Arctic Ocean surface circulation, along with the effects attendant on this process, thus require further study.

Declaration of Competing Interest

The authors declare no conflict of interest.

Acknowledgments

Ocean Reanalysis System 4 (ORAS4) data from the European Centre for Medium-Range Weather Forecasts (ECMWF) are highly appreciated. This research was supported by the National Natural Science Foundation of China (U1901215), the Marine Special Program of Jiangsu Province in China (JSZRHYKJ202007), the Natural Scientific Foundation of Jiangsu Province (BK20181413), and the State Key Lab Fund for Geological Processes and Mineral Resources (2016).

References

Armitage, T.W.K., Bacon, S., Kwok, R., 2018. Arctic Sea Level and Surface Circulation Response to the Arctic Oscillation. Geophys. Res. Lett. 45 (13), 6576–6584.
Balmaseda, M.A., Mogensen, K., Weaver, A.T., 2012. Evaluation of the ECMWF ocean reanalysis system ORAS4. Q. J. R. Meteorol. Soc. 139 (674), 1132–1161.
Chen, X., et al., 2019. Weakened potential vorticity barrier linked to recent winter arctic sea ice loss and midlatitude cold extremes. J. Clim. 32 (14), 4235–4261.
Chepurin, G.A., Carton, J.A., 2012. Subarctic and Arctic Sea surface temperature and its relation to ocean heat content 1982-2010. J. Geophys. Res. Oceans 117 (C6), C06019.
Dommenget, D., Latif, M., 2002. A Cautionary note on the Interpretation of EOFs. J. Clim. 15 (2), 216–225.
Feng, J., Zhang, Y., Cheng, Q., Liang, X.S., Jiang, T., 2019. Analysis of summer Antarctic Sea ice anomalies associated with the spring Indian Ocean dipole. Glob. Planet. Chang. 181 (2019), 102982.
Grinsted, A., Moore, J.C., Jevrejeva, S., 2004. Application of the cross wavelet transform and wavelet coherence to geophysical time series. Nonlinear Process. Geophys. 11 (5/6), 561–566.
Ji, C., Zhang, Y., Cheng, Q., Li, Y., Jiang, T., Liang, X.S., 2018. On the relationship between the early spring Indian's sea surface temperature (SST) and the Tibetan Plateau atmospheric heat source in summer. Glob. Planet. Chang. 164 (2018), 1–10.
Karcher, M., Smith, J.N., Kauker, F., Gerdes, R., Smethie, W.M., 2012. Recent changes in Arctic Ocean circulation revealed by iodine-129 observations and modeling. J. Geophys. Res. Oceans 117 (C8), C08007.
Krishfield, R.A., et al., 2014. Deterioration of perennial sea ice in the Beaufort Gyre from 2003 to 2012 and its impact on the oceanic freshwater cycle. J. Geophys. Res. Oceans 119 (2), 1271–1305.
Li, M., et al., 2020. Anchoring of atmospheric teleconnection patterns by Arctic Sea ice loss and its link to winter cold anomalies in East Asia. Int. J. Climatol. 41 (1), 547–558.
Lorenz, E.N., 1956. Empirical Orthogonal Functions and Statistical Weather Prediction. Massachusetts Institute of Technology, Department of Meteorology, issue 1 of Science Report.
Luo, B., Luo, D., Wu, L., Zhong, L., Simmonds, I., 2017. Atmospheric circulation patterns which promote winter Arctic Sea ice decline. Environ. Res. Lett. 12 (5).
Luo, B., Wu, L., Luo, D., Dai, A., Simmonds, I., 2018a. The winter midlatitude-Arctic interaction: effects of North Atlantic SST and high-latitude blocking on Arctic Sea ice and Eurasian cooling. Clim. Dyn. 52 (5–6), 2981–3004.
Luo, D., Chen, X., Dai, A., Simmonds, I., 2018b. Changes in atmospheric blocking circulations linked with winter arctic warming: a new perspective. J. Clim. 31 (18), 7661–7678.
Ma, B., Steele, M., Lee, C.M., 2017. Ekman circulation in the Arctic Ocean: beyond the Beaufort Gyre. J. Geophys. Res. Oceans 122 (4), 3358–3374.
Maslanik, J.A., Serreze, M.C., Barry, R.G., 1996. Recent decreases in Arctic summer ice cover and linkages to atmospheric circulation anomalies. Geophys. Res. Lett. 23 (13), 1677–1680.
Morison, J., Steele, M., Andersen, R., 1998. Hydrography of the upper Arctic Ocean measured from the nuclear submarine U.S.S. Pargo. Deep Sea Res. Part I Ocean. Res. Pap. 45 (1), 15–38.
Morison, J., et al., 2012. Changing Arctic Ocean freshwater pathways. Nature 481 (7379), 66–70.
Nakamura, T., et al., 2015. A negative phase shift of the winter AO/NAO due to the recent Arctic Sea-ice reduction in late autumn. J. Geophys. Res.-Atmos. 120 (8), 3209–3227.
Nghiem, S.V., et al., 2007. Rapid reduction of Arctic perennial sea ice. Geophys. Res. Lett. 34 (19), L19504.
North, G.R., Bell, T.L., Cahalan, R.F., Moeng, F.J.J.M.W.R., 1982. Sampling Errors in the Estimation of Empirical Orthogonal Functions. Mon. Weather Rev. 110 (7), 699–706.
Overland, J.E., Francis, J.A., Hanna, E., Wang, M., 2012. The recent shift in early summer Arctic atmospheric circulation. Geophys. Res. Lett. 39 (19), L19804.
Pearson, K., 1895. Note on Regression and Inheritance in the Case of two parents. Proc. R. Soc. Lond. 58 (1854–1905), 347–352.
Polyakov, I.V., Johnson, M.A., 2000. Arctic decadal and interdecadal variability. Geophys. Res. Lett. 27 (24).
Proshutinsky, A.Y., Johnson, M., 2001. Two Regimes of the Arctic's Circulation from Ocean Models with Ice and Contaminants. Mar. Pollut. Bull. 43 (1/6), 61–70.
Proshutinsky, A., Bourke, R.H., McLaughlin, F.A., 2002. The role of the Beaufort Gyre in Arctic climate variability: Seasonal to decadal climate scales. Geophys. Res. Lett. 29 (23), 15–1-NaN-15–4.
Rigor, I.G., Wallace, J.M., Colony, R.L., 2002. Response of Sea Ice to the Arctic Oscillation. J. Clim. 15 (18), 2648–2663.
Rudeva, I., Simmonds, I., 2021. Midlatitude Winter Extreme Temperature events and Connections with Anomalies in the Arctic and Tropics. J. Clim. 34 (10), 3733–3749.
Screen, J.A., Bracegirdle, T.J., Simmonds, I., 2018. Polar climate Change as Manifest in Atmospheric Circulation. Curr. Clim. Change Rep. 4 (4), 383–395.
Serreze, M.C., Carse, F., Barry, R.G., Rogers, J.C., 1995. Icelandic Low Cyclone activity: Climatological Features, Linkages with the NAO, and Relationships with recent changes in the Northern Hemisphere Circulation. J. Clim. 10 (3), 453–464.
Simmonds, I., Li, M., 2021. Trends and Variability in Polar Sea Ice, Global Atmospheric Circulations, and Baroclinicity. Ann. N. Y. Acad. Sci. https://doi.org/10.1111/nyas.14673.
Simmonds, I., Burke, C., Keay, K., 2008. Arctic climate Change as Manifest in Cyclone Behavior. J. Clim. 21 (22), 5777–5796.
Steele, M., 2004. Circulation of summer Pacific halocline water in the Arctic Ocean. J. Geophys. Res. 109 (C2).
Steele, M., Ermold, W., Zhang, J., 2008. Arctic Ocean surface warming trends over the past 100 years. Geophys. Res. Lett. 35 (2).
Sun, L., Deser, C., Tomas, R.A., 2015. Mechanisms of Stratospheric and Tropospheric Circulation Response to projected Arctic Sea Ice loss*. J. Clim. 28 (19), 7824–7845.
Thompson, D.W.J., Wallace, J.M., 1998. The Arctic oscillation signature in the wintertime geopotential height and temperature fields. Geophys. Res. Lett. 25 (9), 1297–1300.

Thompson, D., Wallace, J.M., 2001. Regional climate Impacts of the Northern Hemisphere Annular Mode. Science 293 (5527), 85–89.
Timmermans, M.L., Marshall, J., 2020. Understanding Arctic Ocean Circulation: a Review of Ocean Dynamics in a changing climate. J. Geophys. Res. Oceans 125 (4).
Timokhov, L.A., et al., 2018. Climatic changes in the Dynamic Topography and Geostrophic Circulation of the Arctic Ocean. Dokl. Earth Sci. 480 (1), 685–688.
Torrence, C., Compo, G.P., 1998. A Practical Guide to Wavelet Analysis. Bull. Am. Meteorol. Soc. 79 (1).
Wadley, M.R., Bigg, G.R., 2002. Impact of flow through the Canadian Archipelago and Bering Strait on the North Atlantic and Arctic circulation: an ocean modelling study. Q. J. R. Meteorol. Soc. 128 (585), 2187–2203.
Wang, J., et al., 2009. Is the Dipole Anomaly a major driver to record lows in Arctic summer sea ice extent? Geophys. Res. Lett. 36 (5).
Wang, Z., et al., 2015. Variability of sea surface height and circulation in the North Atlantic: Forcing mechanisms and linkages. Prog. Oceanogr. 132, 273–286.
Wu, B., Wang, J., Walsh, J.E., 2004. Dipole anomaly in the winter arctic atmosphere and its association with sea ice motion. J. Clim. 19 (2), 210–225.
Xu, M., Tian, W., Zhang, J., Wang, T., Qie, K., 2021. Impact of Sea Ice Reduction in the Barents and Kara Seas on the Variation of the East Asian Trough in late Winter. J. Clim. 34 (3), 1081–1097.
Yang, X.-Y., Yuan, X., Ting, M., 2016. Dynamical link between the Barents–Kara Sea Ice and the Arctic Oscillation. J. Clim. 29 (14), 5103–5122.
Zhong, W., Zhao, J., Shi, J., Cao, Y., 2015. The Beaufort Gyre variation and its impacts on the Canada Basin in 2003–2012. Acta Oceanol. Sin. 34 (7), 19–31.
Zhong, W., Steele, M., Zhang, J., Cole, S.T., 2019. Circulation of Pacific Winter Water in the Western Arctic Ocean. J. Geophys. Res. Oceans 124 (2), 863–881.